

RESEARCH ARTICLE

Separations: Materials, Devices and Processes

Thermodynamic efficiency of membrane-assisted distillation processes

Bettina Kruber^{1,2} | Karen Droste² | Mirko Skiborowski¹

¹Institute of Process Systems Engineering, Hamburg University of Technology, Hamburg, Germany

²Laboratory of Fluid Separations, Department of Biochemical and Chemical Engineering, TU Dortmund University, Dortmund, Germany

Correspondence

Mirko Skiborowski, Institute of Process Systems Engineering, Hamburg University of Technology, Am Schwarzenberg-Campus 4, 21073 Hamburg, Germany.
Email: mirko.skiborowski@tuhh.de

Abstract

Membrane processes are considered as comparably mild separation processes offering the potential for significant energy savings compared with azeotropic distillation processes. Despite higher investment and material costs, they are of particular interest for improving the energy efficiency in the chemical industry. However, energy savings of more than 20%–30% are rarely reported and even a general superiority can be disputed. To further elucidate this controversial, the current study pursues a quantitative assessment of the thermodynamic efficiency of pervaporation and vapor permeation processes with stand-alone distillation and hybrid membrane-assisted distillation processes for the separation of azeotropic mixtures. The results confirm the case-dependent potential of distillation processes to outperform membrane-assisted separations in terms of energy efficiency, considering proper heat integration. Although energy efficiency is becoming significantly important, it should be considered in the context of economic performance to determine an optimal trade-off and to select the best process alternative during conceptual process design.

KEYWORDS

exergy analysis, optimization, pervaporation, thermodynamic efficiency, vapor permeation

1 | INTRODUCTION

While distillation is a mature and well-known technology, it is generally considered energy intensive and of limited use for the separation of azeotropic mixtures, requiring either pressure-variations or properly selected solvents, which have to be recycled. Membrane processes on the other hand are not limited by vapor–liquid equilibrium and potentially offer high selectivity as well as a compact modular design, given sufficient molecular differences and the availability of suitable membrane. Hybrid separation processes combine at least two unit

operations, which contribute to a common separation task.¹ The integration of various techniques allows to exploit synergetic effects and to overcome limitations of the individual unit operation. Hybrid processes combining distillation and membrane processes belong to the most prominent hybrid processes allowing for the separation of close-boiling or azeotropic mixtures.^{2–4} Especially the combination of pervaporation (PV) or vapor permeation (VP) with distillation have been subject to several publications.^{5–9} The review articles of Lipnizki et al.² as well as Liu et al.¹⁰ give an elaborate overview of possible applications.

Although hybrid separation processes offer a significant potential for performance improvement, the design of a flowsheet structure is a challenging task as a high number of operational and design degrees of freedom has to be considered.⁴ The latter is caused by various

Abbreviations: ED, extractive distillation; NRTL, non-random two-liquid; MED, minimum energy demand; MESH, mass balances, equilibrium conditions, summation constraints and enthalpy balances; PSD, pressure-swing distillation; PV, pervaporation; TAC, total annual costs; THF, tetrahydrofuran; VP, vapor permeation; VLE, vapor–liquid equilibrium.

This is an open access article under the terms of the [Creative Commons Attribution-NonCommercial](https://creativecommons.org/licenses/by-nc/4.0/) License, which permits use, distribution and reproduction in any medium, provided the original work is properly cited and is not used for commercial purposes.

© 2023 The Authors. *AIChE Journal* published by Wiley Periodicals LLC on behalf of American Institute of Chemical Engineers.

possibilities for the combination and interconnection of potential unit operations resulting in various alternatives. In order to identify the best performing configuration, it is advantageous to perform a preliminary screening of promising process variants by applying evaluation criteria based on simplified calculations that are especially important for membrane processes. A prominent screening procedure is based on the driving force for each unit operation as described by Bek-Pedersen et al.^{11,12} who provide a graphical method for the synthesis and design of distillation-based processes. However, application of the graphical approach is limited to binary mixtures or requires the selection of adequate key components.

Further evaluation criteria regard the energy consumption or the economic viability of a process, which are based on the costs of the involved unit operations including investment and operating costs. The latter one can be easily estimated by mass and energy balances, but the accurate determination of investment costs requires in-depth information for a proper sizing of the equipment. Therefore, each unit operation must be described in sufficient detail. Shortcut calculations are very efficient and robust for the determination of the minimum energy requirement,¹³ while rigorous optimization models are applied if an economically optimal process is to be identified.¹⁴ In any case, the estimate of the resulting costs depends strongly on the level of detail the process is described and the accuracy of the cost and sizing correlations. However, for a large number of process alternatives, a high computational effort and a lot of information, especially on the membrane process, are required. At the initial stage of conceptual design, suitable flux models describing the membrane performance are often not available, while acquisition of that information requires experimental investigations.¹⁵

In contrast, the minimum energy demand (MED) of a membrane-assisted process can already be determined accurately at an early conceptual design phase. The MED is often regarded as a measure for operating costs, commonly applied to heat-driven processes, such as distillation.¹⁶ Therefore, only the reboiler duty is considered, while the condenser duty plays a minor role if air cooling or cooling water can be used. For a membrane-assisted process, especially the membrane replacement adds considerable operating costs. Here, the MED of an optimized and approximately ideal process provides a lower bound for the potential performance of the membrane-assisted process. For PV-assisted processes, Scharzec et al.¹⁵ considered the MED for a first assessment of potential processes variants prior to any experimental investigations or detailed rigorous optimization. While this evaluation serves as initial criteria for the justification of costly experiments, it does not distinguish between different energy forms, such as heat or electricity, or temperature levels. Especially for membrane-assisted distillation processes this approach is often impractical as both energy forms are involved and especially pressure-driven membrane processes operate at low temperatures.

To overcome this limitation, an exergy analysis can be conducted to determine the thermodynamic efficiency of a process, which considers the minimum and the actual work of separation. The term “exergy,” also called availability,¹⁷ was first introduced by Zoran¹⁸ in 1956 and describes the maximum useful work which a system can provide when it is brought to equilibrium with its surroundings in reversible mode.¹⁹ Therefore, the process is related to the temperatures of the

heat source and heat sink as well as the thermodynamic pathways. Thus, not only the specific form of energy is considered but also the temperatures at which heat is introduced or removed. Such thermodynamic analysis is a common tool for evaluating individual processes, as well as identifying and quantifying inefficiencies. Demirel¹⁹ provides a comprehensive overview of conventional approaches for thermodynamic analysis with a focus on distillation operations, providing elaborate derivation of the underlying thermodynamic equations. In the following, a short overview of recent applications in the field of distillation and membrane processes is given.

Agrawal and Woodward²⁰ performed exergy analysis of a distillation system for cryogenic air separation to identify process inefficiencies. Later, Agrawal and Herron²¹ and Bandyopadhyay²² analyzed the effect of feed conditions for the thermodynamic efficiency of distillation columns for ideal and non-ideal binary systems, respectively. The first approach was further extended by Agrawal and Fidkowski²³ to investigate ternary distillation configurations, including basic sequences as well as thermally coupled column configurations for the separation of ideal mixtures. Further studies have dealt with energy- and heat-integrated distillation systems, respectively.^{24–26} Similar to Agrawal and Herron,²¹ Blahušiak et al.²⁷ investigated the influence of the feed composition for binary separations in order to derive recommendations for improving the thermodynamic efficiency of distillation-based separations.

While numerous applications for distillation-based separations have been presented, there are only few publications that address membrane processes. Detailed investigations focus on reverse osmosis²⁸ and gas permeation.²⁹ Cussler and Dutta³⁰ considered the maximum possible thermodynamic efficiency of gas permeation and reverse osmosis under simplified assumptions of ideal separations, avoiding complex thermodynamic models. Castel and Favre³¹ analyzed non-selective membrane separations, considering impure product streams. The analysis of minimum as well as real work requirements were demonstrated for the separation of a perfect gas mixture (air) and a non-ideal liquid mixture (seawater). Furthermore recent studies by the group of Agrawal^{32,33} applied thermodynamic efficiency to compare distillation with selected gas permeation and reverse osmosis, respectively. While the thermodynamic efficiency of VP has not been thoroughly investigated in literature (to the best of our knowledge), an exergy analysis of PV and distillation has been conducted by Ishida and Nakagawa,³⁴ who evaluated ideal and non-ideal binary systems by a graphical tool, a so-called energy utilization diagram.

Within this work, we perform a thermodynamic analysis of PV/VP and distillation-based hybrid processes, building on a derivation of the real work of separation for each process. For this purpose, only a few simplified assumptions are made regarding, for example, driving force reducing effects. However, non-ideal mixtures are considered with a specific selectivity for the membrane separation. The current study is supposed to introduce thermodynamic efficiency as additional criteria for the evaluation of PV/VP-assisted distillation processes. This evaluation is therefore supposed to bridge the gap between an energy-based and cost-based evaluation, which requires equipment selection and specification of available utilities, allowing for a more representative

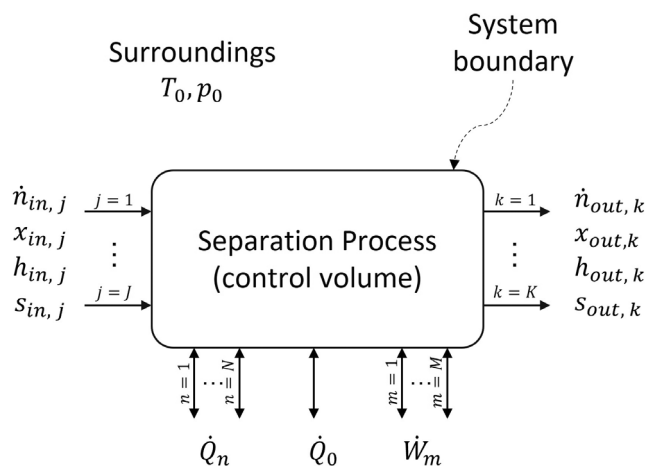


FIGURE 1 Schematic of a separation process with $j = 1, \dots, J$ inlet and $k = 1, \dots, K$ outlet streams, $n = 1, \dots, N$ heat and $m = 1, \dots, M$ work streams related to its surroundings at reference state

evaluation of hybrid processes in an early design phase with consideration of the respective type of energy required. Therefore, a thermodynamic efficiency is determined for the individual configurations based on the performance of the overall process considering optimal process design. Especially, the following questions will be addressed:

- How do membrane processes perform in respect to exergy losses compared to distillation processes and are they generally more efficient?
- Can the thermodynamic efficiency be improved by membrane-assisted hybrid processes?
- How does the thermodynamic efficiency relate to performance metrics such as energy requirements and costs?

The computation of the thermodynamic efficiency of the individual processes is described in Section 2. In a first step, the standalone performance of PV and VP is evaluated in comparison to a distillation process in Section 3, examining the influence of different feed and product compositions. Section 4 assess the applicability of the thermodynamic efficiency as evaluation criterion for PV/VP-assisted hybrid processes by comparing the determined efficiencies with the results of the MED analysis and cost optimization. Section 5 finally presents the respective conclusions and an outlook on future work.

2 | METHODOLOGY

As depicted in Figure 1, we consider a separation process with a defined system boundary with $j = 1, \dots, J$ inlet and $k = 1, \dots, K$ outlet streams, separated from the surrounding reservoir with reference temperature T_0 and pressure p_0 . Mixing of components is a spontaneous irreversible process generating entropy, while the ideal separation of a mixture can be regarded as a reverse mixing process that requires external work to be accomplished, for example, by adding higher potential shaft or heat work,²⁷ which are denoted as \dot{W}_m and \dot{Q}_n ,

respectively. While the latter refers to a respective temperature T_n , \dot{Q}_0 represents the heat stream at reference temperature T_0 , which, however, is eliminated in the derivation of the exergy in Section 2.2. In the following, work and heat streams leaving the system follow the rules of mechanics and are considered negative.

In order to determine the thermodynamic efficiency of a given separation process, we refer to the definition of King³⁵ as the ratio of the minimum (reversible) work \dot{W}_{min} to the real (actual) work \dot{W}_{real} , which can be calculated for any type of separation processes:

$$\eta = \frac{\dot{W}_{min}}{\dot{W}_{real}} = \frac{\dot{W}_{min}}{\dot{W}_{min} + \dot{W}_{irr}}. \quad (1)$$

This definition is in line with the preceding publications.^{21,26,30} The minimum work is the lower bound for the energy requirement of any separation process, while the real work is generally larger resulting in values of the thermodynamic efficiency between zero and one. The real work is the sum of the minimum work and the irreversible losses in the process \dot{W}_{irr} , cf. Section 2.2.³¹

2.1 | Minimum work

The minimum work \dot{W}_{min} is calculated assuming a reversible, isothermal and isobaric process, which does not depend on the specific separation unit but solely on the composition, temperature and pressure of the mixture to be separated as well as the respective product streams.³⁵ For such a process, the minimum work can be calculated by an exergy balance accounting for the inlet and outlet streams as demonstrated by Agrawal and Woodward²⁰ or Demirel.¹⁹ The exergy of a material stream comprises of a physical, chemical, kinetic and potential part of the exergy. For a classical separation process, no chemical reaction is considered, and the kinetic and potential exergy can be neglected, which results in the following expression

$$\dot{W}_{min} = \sum_k \dot{n}_{out,k} (h_{out,k} - T_0 s_{out,k}) - \sum_j \dot{n}_{in,j} (h_{in,j} - T_0 s_{in,j}) \quad (2)$$

with h being the enthalpy and s the entropy of the inlet and outlet material streams. At ambient conditions, this term equals the negative Gibbs free energy of mixing ΔG_{mix} ^{28,32} and represents the work required to reverse the mixing process. Thus, the minimum work can also be determined by Equation (3) assuming liquid inlet and outlet streams.

$$\begin{aligned} \dot{W}_{min} &= -\Delta G_{mix}(T_0, p_0) \\ &= -RT_0 \left[\sum_j \dot{n}_{in,j} \sum_i x_{in,i} \ln(x_{in,i} \gamma_{in,i}) - \sum_k \dot{n}_{out,k} \sum_i x_{out,i} \ln(x_{out,i} \gamma_{out,i}) \right]. \end{aligned} \quad (3)$$

Here, x_i is the molar fraction and γ_i the activity coefficient of component i of the inlet and outlet material stream, respectively. This equation is applicable to non-ideal mixtures with $j = 1, \dots, J$ inlet streams which are separated into $k = 1, \dots, K$ (possibly impure) product

streams. The assumption of ideal mixtures and pure product streams leads to considerable simplifications of the equation. Refer, for example, to the work of Agrawal and Herron²¹ for the respective derivations.

2.2 | Real work

The real work is derived following Demirel,¹⁹ building on the first law (energy balance) and second law of thermodynamics (entropy balance). Equation (4) gives a general energy balance for a control volume assuming steady state conditions and negligible kinetic and potential energy.

$$0 = \sum_j \dot{n}_{in,j} h_{in,j} - \sum_k \dot{n}_{out,k} h_{out,k} + \dot{Q}_0 + \sum_n \dot{Q}_n + \sum_m \dot{W}_m. \quad (4)$$

The first terms are the enthalpy flow rates of the inlet and outlet streams, \dot{Q}_0 is a heat stream from the surrounding at temperature T_0 , \dot{Q}_n are heat streams at temperature T_n and \dot{W}_m are work contributions to the system, including mechanical, expansion, contraction or electrical work. Equation (5) gives the entropy balance for the control volume assuming steady state conditions, where \dot{S}_{irr} is the rate of entropy production due to irreversibilities.

$$\dot{S}_{irr} = \sum_j \dot{n}_{in,j} h_{in,j} - \sum_k \dot{n}_{out,k} h_{out,k} + \frac{\dot{Q}_0}{T_0} + \sum_n \frac{\dot{Q}_n}{T_n}. \quad (5)$$

Combining the energy balance, Equation (4), with the entropy balance, Equation (5), yields an exergy balance as derived in Equation (6).

$$T_0 \dot{S}_{irr} = \sum_j \dot{n}_{in,j} (h_{in,j} - T_0 s_{in,j}) - \sum_k \dot{n}_{out,k} (h_{out,k} - T_0 s_{out,k}) + \sum_n \dot{Q}_n \left(1 - \frac{T_0}{T_n}\right) + \sum_m \dot{W}_m. \quad (6)$$

The first terms on the right side of the equation are the exergy flow rates of the material streams representing the negative minimum work ($-\dot{W}_{min}$) as described in Equation (2). The product of the reference temperature and the produced entropy ($T_0 \dot{S}_{irr}$) is called lost work or exergy loss and corresponds to \dot{W}_{irr} in Equation (1), which relates the evolution of the control volume to the conditions of the surroundings. The real work of separation is the sum of the reversible and lost work and can be expressed by Equation (7). The first term of the right side of the equation corresponds to the exergy of heat streams, while the second term summarizes the external work on the system.

$$\dot{W}_{real} = \dot{W}_{min} + \dot{W}_{irr} = \sum_n \dot{Q}_n \left(1 - \frac{T_0}{T_n}\right) + \sum_m \dot{W}_m. \quad (7)$$

2.3 | Real work of process units

While the minimum work is independent of the specific separation process, the real work has to be calculated individually for each unit

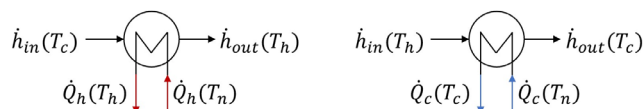


FIGURE 2 Schematic of a reboiler (left) and a condenser (right) to describe heat exchangers contributing to the real work

as it depends on operating conditions and process design. For the considered separation processes (distillation, PV, and VP), we specify the system boundaries as well as work and heat contributions according to Equation (7) including assumptions made for the specific units as well as for the auxiliary equipment, such as heat exchangers, pumps and compressors. Based on these individual considerations, hybrid process configurations can be generated and evaluated. To guarantee comparability of the processes, equal reference conditions of the inlet and outlet material streams are assumed and warranted through integration of additional auxiliary equipment.

2.3.1 | Auxiliary equipment

To determine the exergy loss of a heat exchanger, the temperature of the heating or cooling utility (T_n) is required as defined in Equation (7). This is illustrated in Figure 2 with \dot{Q} being the heat flowrate and \dot{h}_{in} and \dot{h}_{out} the in- and outgoing enthalpy flowrates. In case of external heating, the minimum work required corresponds to a hot stream that supplies \dot{Q}_h at the temperature T_h , at which the heated stream will leave the heat exchanger. This results in zero temperature driving force and thus minimum exergy loss in the heat exchanger. For cooling, the maximum work that can be utilized from the released heat \dot{Q}_c is obtained at temperature T_c , which corresponds to the outlet temperature of the cooled stream. This again results at zero temperature driving force and respective minimum exergy loss in the heat exchanger.

While these assumptions would result in infinitely large condenser and reboiler areas due to the vanishing temperature driving force, any increase in the hot utility temperature or decrease in the cold utility temperature would induce additional external exergy losses in the heat exchangers, which would diminish the thermodynamic efficiency of the separation processes.²⁶

For the sake of the current study, we focus on the comparison of the (internal) efficiency of the considered separation processes, deliberately selecting this rather optimistic assumption for the utility temperatures, pointing out that the subsequently reported results are reflective of this decision. However, practical (external) efficiencies of the processes will be lower accounting for exergy losses in the heat exchangers due to increased hot utility temperatures and decreased cold utility temperatures. The article of Tumbalam Gooty et al.,²⁶ which evaluates the thermodynamic efficiencies of distillation columns and potential means for their improvement, provides an illustrative quantitative example that evaluates the effect of different utility temperatures for the heat exchangers of a distillation column.

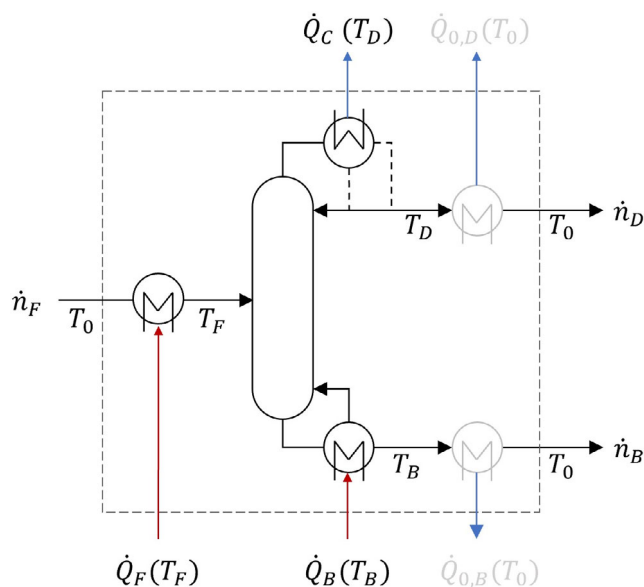


FIGURE 3 Schematic of a distillation unit (worst-case scenario) with all heat and work streams contributing to the real work related to its surroundings at reference state. Gray heat exchangers do not contribute to the real work.

The required work to change the pressure p from a certain state 1 to state 2 of a volume V can be described by the integral given in Equation (8).

$$W_p = \int_1^2 V dp. \quad (8)$$

Assuming an incompressible fluid, the compression and relaxation work stream is given by

$$\dot{W}_{p,L} = \dot{V}(p_2 - p_1), \quad (9)$$

while for a vaporous stream, an ideal gas can be assumed resulting in

$$\dot{W}_{p,G} = \dot{n}RT \ln\left(\frac{p_2}{p_1}\right) \quad (10)$$

with \dot{n} being the molar flow, R the ideal gas constant, T the temperature and p the pressure.

2.3.2 | Distillation

Assuming that the ingoing and outgoing streams are at reference conditions, only exergy in form of heat has to be considered to determine the real work of the distillation process, as illustrated in Figure 3. The feed is preheated to the operating conditions of the column assuming a boiling liquid, while the bottom and top stream are partially evaporated and (fully or partially) condensed, respectively. Both product streams leave the distillation column at different temperatures than

the reference temperature T_0 , requiring an additional heat exchanger to adjust the temperature. Determining the exergy of the product streams for the temperature that is finally reached (cf. Section 2.3.1), the respective exergy flowrate in Equation (7) becomes zero in case of the reference temperature ($T_n = T_0$). Both heat exchangers are depicted in gray in Figure 3, indicating that they have no influence on the real work under this assumption.

Accordingly, the real work is composed of the heat contributions presented in Equation (11). Here, the preheating as well as the reboiler duty are positive, while the condenser duty is negative, which gives a discount on the real work of separation.

$$\dot{W}_{real,dis} = \dot{Q}_F \left(1 - \frac{T_0}{T_F}\right) + \dot{Q}_B \left(1 - \frac{T_0}{T_B}\right) + \dot{Q}_C \left(1 - \frac{T_0}{T_D}\right). \quad (11)$$

Although we are not considering additional temperature differences for utilities and respective external exergy losses for the heat exchangers, we refer to this scenario as “worst case,” since the usable heat of the product streams is discarded to the environment and external heat is used to preheat the feed. The required heat \dot{Q}_F is calculated by an enthalpy balance for the heat exchanger. For further comparison, an additional “best-case” efficiency is calculated, considering that the sensible heat of the product streams provides sufficient heat to preheat the feed stream, such that no external preheating is required. This “best case” efficiency corresponds to the analysis performed by Tumbalam Gooty et al.²⁶ and enables a comparison with this analysis. Both assumptions represent limiting values, which can be considered as lower and upper bounds for the thermodynamic efficiency, depending on the actual degree of heat integration. For the best-case scenario, we assume that the product streams provide the necessary amount of heat for preheating ($\dot{Q}_F = 0$), such that the exergy flowrate for the preheater is omitted from Equation (11).

The condenser and reboiler duties, \dot{Q}_C and \dot{Q}_B , depend on the reflux ratio and boil-up rate for the desired separation, requiring data on the energy demand of the distillation column. For this purpose, either experimental data can be used or model-based calculations can be conducted, for example, with shortcut or rigorous models.³¹ Furthermore, for a vacuum or high-pressure distillation process, additional pumps and relaxation valves have to be considered in the feed and product streams, according to Equation (9).

2.3.3 | Pervaporation

In PV processes, a liquid feed enters the membrane unit, while the permeating components evaporates after passing through the membrane due to applied vacuum on the permeate side, resulting in a lower partial pressure of the permeating components than the corresponding saturation pressure. To calculate the real work of PV, the process scheme in Figure 4 is considered. The liquid feed is pumped and preheated to membrane operating conditions p_F and T_{mem} , respectively. The vaporous permeate stream is condensed to saturated liquid conditions and then compressed to the reference pressure

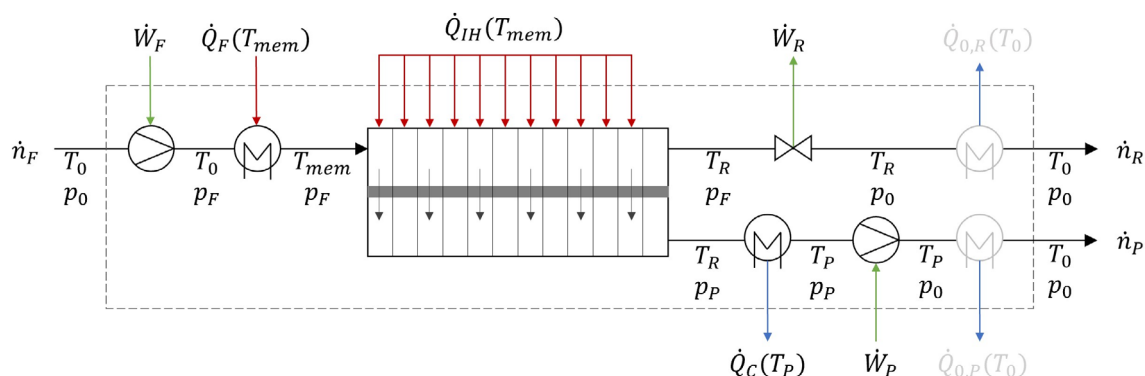


FIGURE 4 Schematic of a PV unit with all heat and work streams contributing to the real work related to its surroundings at reference state. Gray heat exchangers do not contribute to the real work.

p_0 , while the liquid retentate stream is relaxed to p_0 . Both streams are then returned to the reference temperature T_0 by a heat exchanger, which is only indicated in gray as the contribution is again assumed to be zero.

It is important to note, that depending on the permeate pressure and the respective boiling temperature, the real work for the condensation of the permeate can either result in a positive or negative exergy stream. If the boiling temperature is below the reference temperature, the condensation will result in an additional exergy loss, while a boiling point above the reference temperature will provide some discount in the calculated efficiency. This behavior does at least qualitatively reflect the economic burden that a condensation below ambient temperature brings.

PV is characterized by the evaporation of the permeating component(s), which causes a temperature drop on the feed-side along the membrane. Especially for water as permeating component, which is typical for hydrophilic PV membranes, this temperature drop is significant due to the high enthalpy of vaporization. For this reason, intermediate heaters are commonly used. As indicated in Figure 4, such interstage heating is considered by dividing the membrane into n_{disc} elements. Therefore, the total permeate stream is divided by n_{disc} , which represents the partial permeate stream in one discrete element. This way, each element is balanced with the feed stream being the retentate stream of the previous element. Between each element the feed is heated up to the specified membrane operating temperature T_{mem} . The resulting temperature drop is calculated by an energy balance neglecting the heat of mixing³⁶:

$$T_{mem} - T_R = \frac{\dot{n}_P \Delta h_F^{LV}}{\dot{n}_F c_{p,F}}. \quad (12)$$

Considering a constant feed and permeate pressure, the real work of separation is defined by Equation (13), where n_{disc} is defined as the number of permeate streams for the calculation of the intermediate heating and condensation. Considering all illustrated contributions, the real work of PV is defined as follows:

$$\begin{aligned} \dot{W}_{real,PV} = & \dot{V}_F(p_F - p_0) + \dot{Q}_F \left(1 - \frac{T_0}{T_{mem}} \right) + \sum_{n_{disc}-1} \dot{Q}_{IH,j} \left(1 - \frac{T_0}{T_{mem}} \right) \\ & + \dot{V}_R(p_0 - p_F) + \dot{Q}_C \left(1 - \frac{T_0}{T_P} \right) + \dot{V}_P(p_0 - p_{mem}). \end{aligned} \quad (13)$$

For the calculation of the real work, the volume flows \dot{V} of each stream have to be determined. For a specific application, the membrane performance is usually described by a respective flux model based on experimental investigations. However, for an early assessment in conceptual design and in case a proper model is not available, a (nearly) perfect separation into permeate and retentate can be assumed for an initial screening based on a predefined selectivity of the membrane. Thus, the retentate and permeate stream are calculated by mass balances for a given retentate and permeate purity. Experimental investigations can thus be motivated once sufficient potential for the membrane or membrane-assisted separation is determined. The heat duty required for preheating the feed stream is calculated based on the membrane feed temperature, which in this case corresponds to boiling liquid conditions.

While similar to the distillation column, the heat released by retentate cooling could be used to compensate a part of the heat for feed preheating, the permeate stream is first condensed at low temperature due to the low permeate pressure. Thus, for proper heat integration, the vaporous permeate stream would first need to be cooled in a heat exchanger with the feed stream, prior to condensation. Such configuration is rather uncommon as the vacuum on the permeate side is maintained by a vacuum pump attached to the condenser. Therefore, no best-case approximation for feed and product heat integration is considered for the membrane process, although there is potential for improvement of the thermodynamic efficiency by means of such heat integration.

Furthermore, the operating conditions of the membrane, including the pressure of the feed p_F and permeate p_P as well as the operating temperature T_{mem} need to be specified. In order to approximate the minimum energy requirement, a vanishing driving force for the mainly permeating component at the end of the membrane unit is assumed. This would in fact require an infinite membrane area and corresponds to the assumption of an infinite number of equilibrium

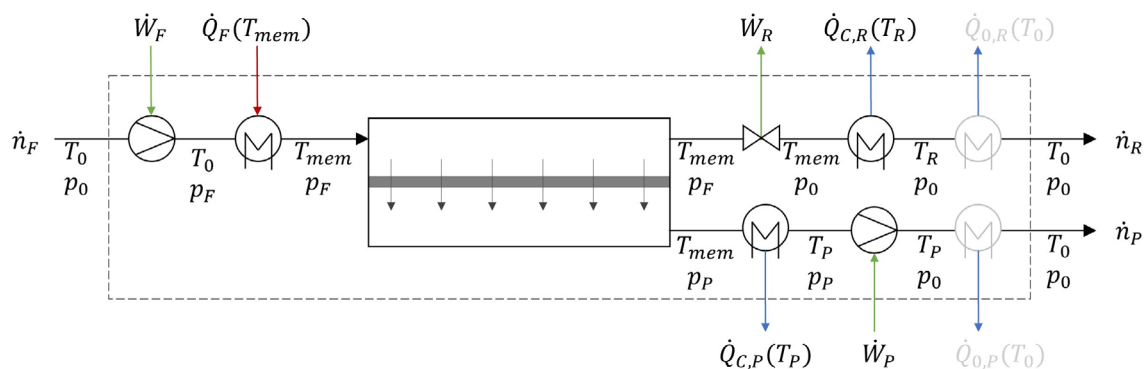


FIGURE 5 Schematic of a VP unit with all heat and work streams contributing to the real work related to its surroundings at reference state. Gray heat exchangers do not contribute to the real work.

stages in distillation for the approximation of the minimum energy requirements.

The driving force of a component i for any membrane process is defined by the difference in the chemical potential between the feed- and permeate-side of the membrane. For PV, the driving force of component i of PV is defined by Equation (14).³⁶

$$\Delta\mu_{i,PV} = RT \ln \frac{x_{i,F} \gamma_{i,F} p_{0,i}^S \varphi_{0,i}^{LV}}{y_{i,P} p_P \varphi_{i,P}}. \quad (14)$$

For a fixed permeate pressure, the driving force depends only on the temperature, which cannot be determined explicitly as the vapor pressure $p_{0,i}^S$ as well as the fugacity coefficients $\varphi_{0,i}^{LV}$ and $\varphi_{i,P}$ are functions of the temperature. Ensuring a liquid feed and retentate stream, the feed-side pressure and temperature are determined iteratively until a vanishing driving force is achieved. Therefore, a minimum feed-side pressure is defined as starting point, while the temperature corresponds to the boiling temperature of the feed. Then, the temperature is successively decreased for a constant feed-side pressure. If a vanishing driving force cannot be achieved, the feed-side pressure is increased until the driving force is zero.

2.3.4 | Vapor permeation

VP is characterized by vaporous feed and product streams, which contain only condensable vapors. The contributions to the real work are illustrated in Figure 5 neglecting a possible pressure drop along the membrane. The feed stream is first pumped to the desired feed-side pressure p_F and then evaporated and superheated to reach the membrane operating temperature T_{mem} . Inside the membrane module, isothermal operating conditions are assumed. Thus, the retentate and permeate streams leave the module at temperature T_{mem} .

For the current evaluation, it is considered that the vaporous retentate stream is further relaxed to atmospheric pressure p_0 followed by a condensation to boiling liquid conditions, releasing heat $\dot{Q}_{C,R}$ at temperature T_R and reducing the temperature to ambient conditions, which does not contribute to the real work. Another option

would be to first condense and further subcool the retentate stream prior to relaxation to atmospheric pressure. In this case, the heat of condensation could be released at a higher temperature level resulting in an increased thermodynamic efficiency, which is however not considered here.

The vaporous permeate stream is first condensed to the low-pressure boiling temperature T_P , before pressure and temperature are increased to ambient conditions. Similar to the introduced PV process, the real work for condensation of the permeate can result in a positive or a negative exergy stream depending on the permeate pressure and boiling temperature.

Summarizing the depicted contributions leads to the real work of VP calculated by Equation (15). In case of an already vaporous feed stream, the compression work has to be determined based on Equation (10) instead of Equation (9).

$$\begin{aligned} \dot{W}_{real,VP} = & \dot{V}_F(p_F - p_0) + \dot{Q}_F \left(1 - \frac{T_0}{T_{mem}} \right) + RT_{mem} \dot{n}_R \ln \frac{p_0}{p_F} + \dot{Q}_{C,R} \left(1 - \frac{T_0}{T_R} \right) \\ & + \dot{V}_P(p_0 - p_P) + \dot{Q}_{C,P} \left(1 - \frac{T_0}{T_P} \right). \end{aligned} \quad (15)$$

The volume flows and the description of the membrane performance are determined analogously to PV. For the membrane operating conditions, we again assume a vanishing driving force of the mainly permeating component at the end of the membrane unit. The driving force of component i of VP can be expressed by the difference in partial pressures caused by either a pressure reduction on the permeate-side and/or a pressure increase on the feed-side. Equation (16) shows the driving force for a non-ideal gas considering the molar fractions y_i , the pressures p and the fugacity coefficients φ of the feed- and permeate-side.³⁶

$$\Delta\mu_{i,VP} = RT \ln \frac{y_{i,F} p_F \varphi_F}{y_{i,P} p_P \varphi_P}. \quad (16)$$

For a driving force of zero at the end of the membrane, that is, in the retentate stream, Equation (16) can be written in the following way by setting $\Delta\mu_{i,VP}$ to zero and rearranging it to the permeate pressure:

$$p_P = p_F \frac{Y_{i,R} \varphi_R}{Y_{i,P} \varphi_P} \quad (17)$$

In order to determine the permeate pressure, atmospheric pressure on the feed side is assumed, seeking a net driving force of zero. As the permeate fugacity also depends on the permeate pressure, it is determined iteratively. If the permeate pressure falls below a predefined threshold value, the feed-side pressure is increased instead to reach a vanishing driving force in the retentate outlet stream. The feed temperature is calculated for the resulting feed pressure assuming a saturated vapor. Of course, the feed pressure could be increased first until the maximum allowable pressure of a potential membrane is reached. A higher feed pressure results in a higher feed temperature, which on the one side requires added heat duty to preheat and evaporate the feed stream. On the other side, the flux is doubled by a temperature increase of 20 K,³⁶ such that higher temperatures result in a lower membrane area, which does however not directly affect the thermodynamic efficiency.

2.3.5 | Hybrid processes

For hybrid processes, the same assumptions and equations apply as deduced in the previous sections for heat exchangers, pumps and compressors, distillation columns as well as the considered membrane processes. In case of internal recycle streams, a holistic consideration of the whole process has to be conducted to determine the respective heat and work streams of the units. Hybrid processes are specified in more detail in the respective case studies in Section 4.

3 | INVESTIGATION OF STANDALONE UNITS

Before analyzing the efficiency of a hybrid separation process, the stand-alone unit operations (distillation, VP, and PV) are examined to investigate the influence of the feed composition as well as product purities on the minimum work and the thermodynamic efficiency. While distillation is often referred to as inefficient separation technique, thorough comparisons with other processes are scarce. As pointed out by Cussler and Dutta,³⁰ alternative processes, such as absorption, extraction, or membrane separations, show inefficiencies like those found for distillation, which are more pronounced for separations with high purities and recoveries. These statements are supported by the recent study of Chavez Velasco et al.,³³ who conclude that the general conception that thermal separation processes are inherently energy efficient are ill-founded.

The current investigation allows to identify the maximum possible thermodynamic efficiency of each of the considered separation process and enables a comparison. In industry, PV and VP are primarily applied for the dehydration of alcohols, such as ethanol or isopropanol.³⁷ Especially the dehydration of ethanol is of tremendous importance for the biochemical industry, with an estimated annual

worldwide production of more than a 100 billion liters of bioethanol.³⁸ Therefore, we consider the separation of a binary mixture of ethanol and water with a feed stream of 100 mol s⁻¹ at a reference temperature of 298.15 K and atmospheric reference pressure as a representative case study. At this pressure, the mixture also exhibits an azeotropic point at 89.1 mol% ethanol,³⁹ impeding separation by simple distillation.

For all following investigations within this section, the vapor-liquid equilibria are modeled with the NRTL activity coefficient model and the Redlich-Kwong equation of state combined with the extended Antoine equation. The enthalpies are determined based on DIPPR correlations for the specific heat capacities and heat of vaporization. The parameter sets for the individual models are derived from ASPEN APV-V88 VLE-IG and PURE32 database.

3.1 | Minimum work

The minimum work of a separation process represents the lower bound of the work that must be performed to separate a mixture reversibly and isothermally. This threshold only depends on the mixture to be separated and is thus equal for all considered separation processes. It should be noted that thermodynamic limitations for an individual separation, for example, the azeotropic point, are not taken into account here.

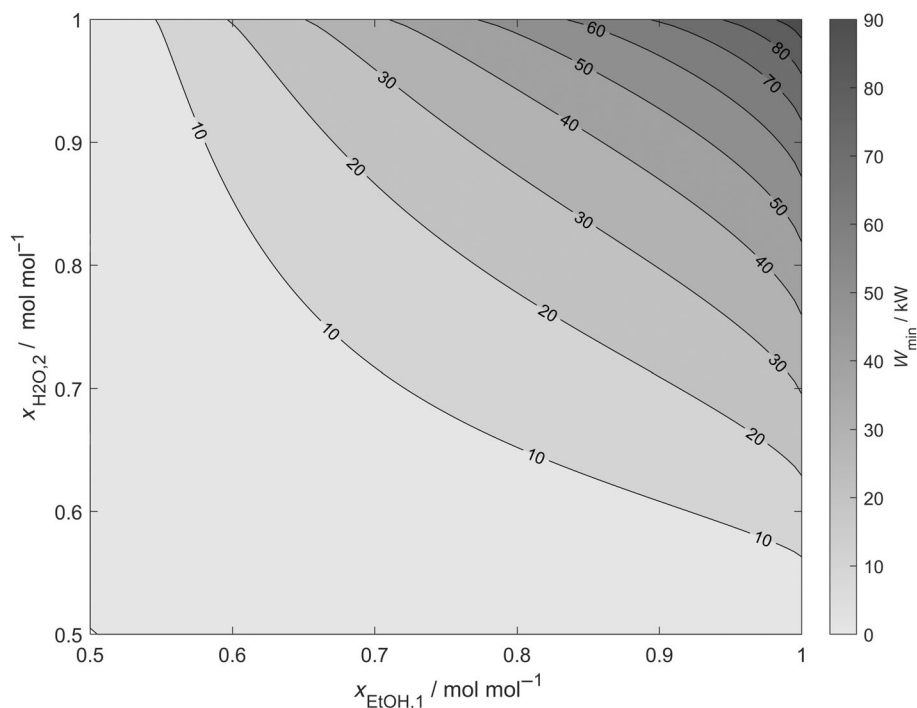
The minimum work is calculated for an equimolar ethanol-water mixture considering the total product range of ethanol and water in the respective product streams as depicted in Figure 6. While ethanol enriches in product stream one, water enriches in product stream two, which could be either the top and bottom stream of a distillation column, or the retentate and permeate stream of a membrane process, respectively. The contour plot shows that the minimum work increases with higher product purities reaching a maximum of almost 100 kW at pure component compositions of both product streams. While a purification of both components to only 70 mol% requires less than 10 kW, a purification to 90 mol% already requires a minimum work of 40 kW steeply rising to 100 kW for high purity products. In contrast, obtaining only one pure component results in a significantly lower energy demand.

The influence of the feed composition on the minimum work was investigated as well, for which the results are presented in the Supplementary Information (Section A.1). The separation of a mixture requires the highest energy for an almost equimolar feed with both products to be obtained in pure state.

3.2 | Thermodynamic efficiency

Based on the previously determined minimum work and the real work calculated with the methods presented in Section 2.3, the thermodynamic efficiency is determined for each presented unit operation. For the distillation process, we compare the best-case with the worst-case scenario extended by an analysis of the considered temperature in the

FIGURE 6 Minimum work in kW for the separation of an equimolar ethanol–water mixture for different product purities (ethanol is enriched in product stream 1, water is enriched in product stream 2) with $T_0 = 298.15$ K, $p_0 = 1.013$ bar, $\dot{n}_F = 100$ mol s⁻¹



heat exchangers. Furthermore, we compare the resulting information on the thermodynamic efficiency with the driving force analysis proposed by Bek-Pedersen and Gani¹² to analyze the correspondence of these methods and identify optimal combinations of unit operations.

3.2.1 | Distillation

To determine the real work of separation for a distillation process, the reboiler and condenser duty is required, as given in Equation (11). Therefore, the distillation column is described with a rigorous equilibrium-stage model, which is based on mass balances, equilibrium conditions, summation constraints and enthalpy balances known as MESH equations. A superstructure model is implemented in GAMS (General Algebraic Modeling System) with equilibrium calculations and additional thermodynamic calculations performed by means of external equations.⁴⁰ To derive the MED of the distillation column, an optimization problem needs to be solved, minimizing the overall energy demand, given the product specifications. For a fixed number of equilibrium stages and a fixed feed position, the design degrees of freedom are the reflux and boil-up ratio. A detailed description of the model equations is described by Skiborowski et al.⁴⁰ For the current investigations, a column with 150 equilibrium stages is considered, resulting in a good approximation of the minimum heat requirements.

Considering the separation of an equimolar ethanol–water mixture, a water-rich stream in the bottom and an ethanol-rich stream in the top of the column are produced. While water can be purified, the ethanol purity of the top product is limited by the azeotropic point. The thermodynamic efficiencies of the distillation process are depicted for the whole range of achievable purities in both product

streams in Figure 7. The worst-case scenario is depicted in the left diagram, while the best-case scenario is shown in the right diagram.

The overall thermodynamic efficiency for the worst-case scenario is generally low with a maximum of 18% in the range of 85 mol% ethanol and water in the distillate and bottom stream, respectively, which is caused by the different trends of the minimum and real work. Although both increase with higher purities of the product streams, the change in minimum work is stronger for purities up to 85 mol%. The diagram for the real work is given in the Supplementary Information (Section A.2). Water compositions in the bottom close to the feed composition achieve efficiencies of only 4%–10%, because the separation work is generally small but the work for preheating the feed of 90 kW (constant for each considered product purity) accounts for more than 50% of the real work.

To determine the best-case efficiency, a full compensation of the heat required for feed preheating by cooling the product streams is assumed, which requires a heat duty of 586 kW to reach the boiling temperature of 79.8°C. Depending on the product purities the product cooling provides sufficient heat duties between 584 and 635 kW, with max. temperatures between 78.2 and 78.9°C for the top product and 79.8 and 99.7°C for the bottom product. Thus, the simplified assumption of a full compensation of the heat duties for feed preheating by cooling of the product streams provides a reasonable upper bound.

The respective results for the best-case scenario are depicted in Figure 8, right. The thermodynamic efficiency rises up to about 70% for low water compositions and ethanol product purities in the range of 75–85 mol%, which is in good agreement with the internal efficiencies reported by Tumbalam Gooty et al.²⁶ for the separation of ideal binary mixtures. The thermodynamic efficiency decreases with higher

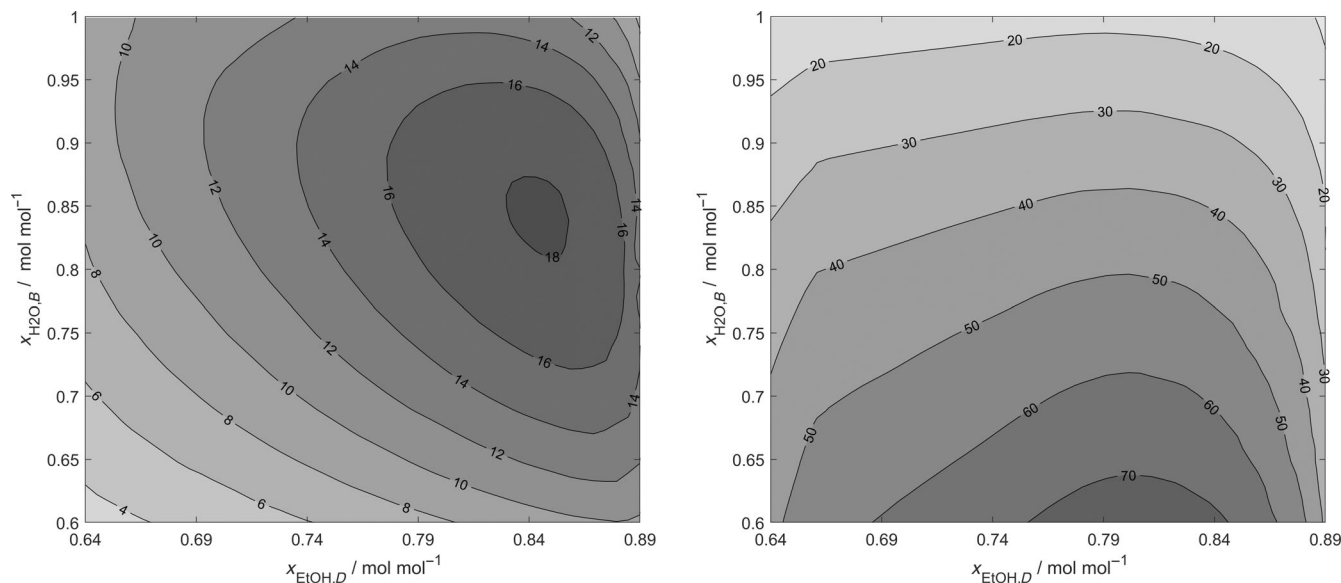


FIGURE 7 Thermodynamic efficiency in % for the worst-case scenario (left) and the best-case scenario (right) of a stand-alone distillation unit of an equimolar ethanol–water mixture for different distillate and bottom compositions with $T_0 = 298.15$ K, $p_0 = 1.013$ bar, $\dot{n}_F = 100$ mol s $^{-1}$

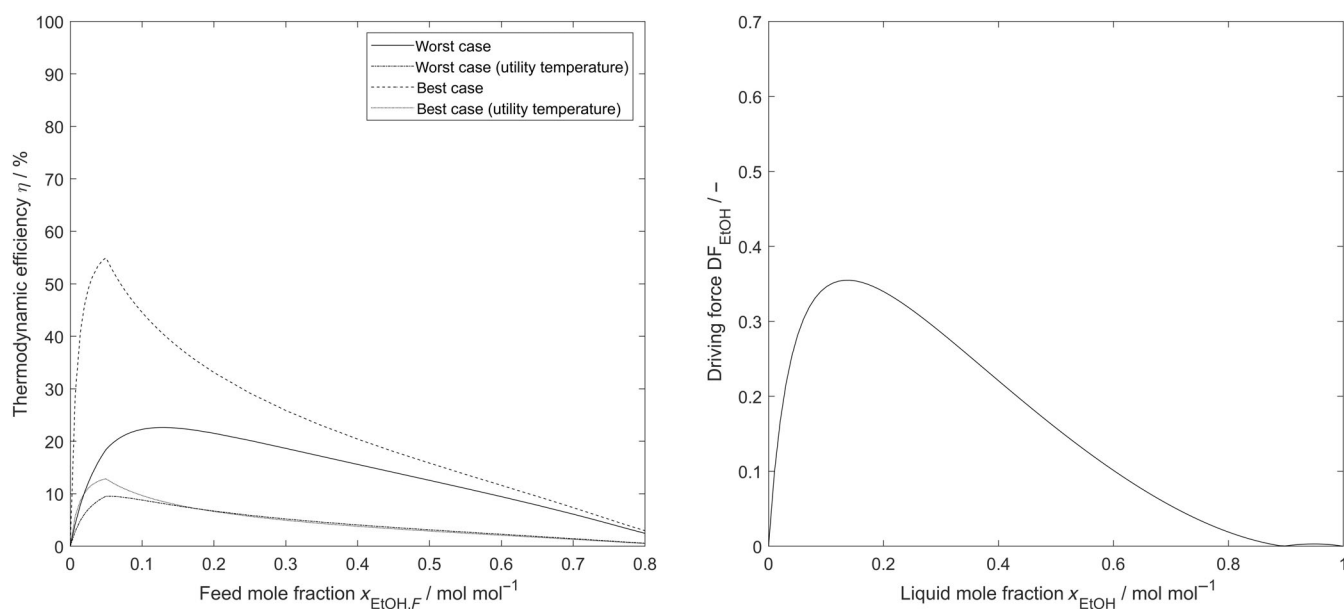


FIGURE 8 Thermodynamic efficiency (left) and driving force according to Bek-Pederson and Gani¹² (right) of a stand-alone distillation unit of ethanol and water for different feed compositions with $x_{\text{EtOH},D} = 0.85$, $x_{\text{H}_2\text{O},B} = 0.999$, $T_0 = 298.15$ K, $p_0 = 1.013$ bar, $\dot{n}_F = 100$ mol s $^{-1}$

water purities in the bottom because more ethanol has to be separated. Approaching the azeotropic point, the thermodynamic efficiency rapidly decreases to values lower than 10% comparable to the worst-case scenario.

It is obvious that heat integration between the hot product streams and the feed stream is of significant importance for maximizing the thermodynamic efficiency of the distillation column. For moderate purities, for example, 85 mol% ethanol and water, the efficiency is doubled, while for high water purities, still an increase of about one third is noticeable. However, for product purities near to

the azeotropic point, both cases exhibit the same low thermodynamic efficiencies indicating that distillation is inefficient for product purities in this range.

The influence of the feed composition on the thermodynamic efficiency is further analyzed for a top product purity of 85 mol% ethanol, close to the azeotrope, and a bottoms product purity of 99.9 mol% water, which is illustrated in Figure 8 (left). For the worst case, a maximum efficiency of about 22% is achieved at a feed composition of 13 mol% ethanol. Approaching the azeotropic composition, the thermodynamic efficiency decreases as the required reboiler

duty increases due to a higher amount of ethanol which has to be evaporated. Generally, the feed compositions close to the product specifications require a small amount of minimum work but the contribution of the feed preheating as well as reboiler duty to the real work is high resulting in low efficiencies. The best-case scenario shows a similar trend but with considerable higher thermodynamic efficiencies. The maximum of 55% exceeds the maximum of the worst case by a factor larger than two, highlighting the importance of utilizing the sensible heat of the product streams through heat integration.

In a second step, the thermodynamic efficiencies are recalculated, considering additional exergy losses in the heat exchangers, due to increased and decreased utility temperatures. Therefore, we consider steam with a temperature of 120°C for evaporation and preheating, as well as cooling water with a temperature of 25°C for condensation. Due to the additional exergy losses, the thermodynamic efficiency is considerably lower with maximum values of 13% and 10% for the best and worst case, respectively. The values differ only slightly as the influence of the preheater is small compared to the condenser and reboiler work. While the exergy flowrate for the reboiler increases to some extent due to the temperature increase from 99.7°C (almost pure water in the bottom stream) to 120°C (saturated steam), the main difference results from the lost discount for the condenser, as the previously utilizable heat at 78.2°C (almost azeotropic composition in the distillate), is lost to the environment at 25°C (cooling water). This further demonstrates the importance of utilizing the latent heat of condensation for the distillation column and the considerable drop in efficiency linked to wasting this energy to the environment, which is also in line with the findings of Tumbalam Gooty et al.²⁶

For all cases, it is apparent that the feed composition has a considerable impact on the efficiency as well, as already presented by Agrawal and Herron,²¹ Bandyopadhyay²² and Tumbalam Gooty et al.²⁶ The same trend is observed for the driving force DF determined by $DF_i = y_i - x_i$ according to Bek-Pedersen and Gani,¹² which is shown in Figure 8 (right) for ethanol. The maximum is obtained at about 14 mol% ethanol, while it decreases to pure water and to the azeotropic point. However, the decline of the thermodynamic efficiency is much less pronounced as the driving force for increasing ethanol fraction in the feed.

3.2.2 | Pervaporation

To investigate the thermodynamic efficiency of PV, the actual work requirement for different product purities of the retentate and permeate stream is analyzed. Considering a hydrophilic membrane, water is the preferentially permeating component and ethanol is obtained in the retentate with variable compositions up to pure ethanol. For the permeate, only two distinct permeate compositions are considered:

- A pure water permeate representative of a high selectivity membrane, such as an NaA zeolite membrane with water/ethanol permselectivity up to 10,000.⁴¹

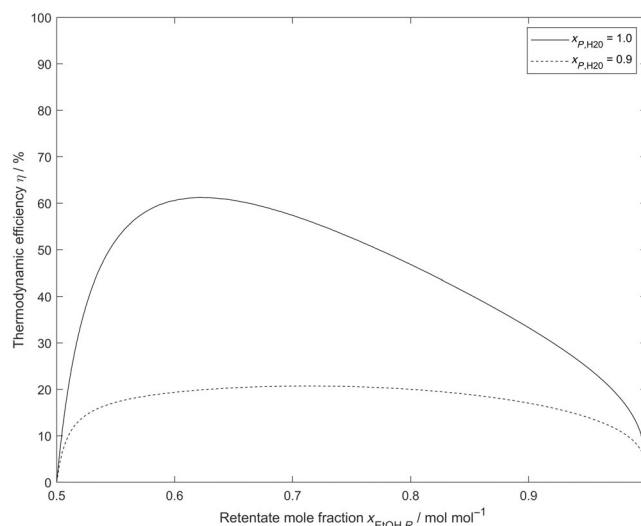


FIGURE 9 Thermodynamic efficiency of a stand-alone PV of an equimolar feed of ethanol and water for different retentate purities with $p_P = 50$ mbar, $T_0 = 298.15$ K, $p_0 = 1.013$ bar, $\dot{n}_F = 100$ mol s⁻¹

- An imperfect membrane with a reduced selectivity resulting in a permeate composition of 90 mol% water.

The permeate pressure should be as low as possible to establish a high flux, while condensation with cooling water should be preferred economically. As both factors affect the economy of PV and are not evaluated within the analysis of the thermodynamic efficiency, a permeate pressure of 50 mbar is selected as representative.

The resulting thermodynamic efficiencies are illustrated in Figure 9, while the respective membrane temperature is given in the Supplementary Information (Section A.3). For a pure permeate, the highest efficiency of 60% is reached at about 62 mol% ethanol, where only a minimal ethanol purification is accomplished. The efficiency decreases constantly for higher water recoveries and respective higher purities in the retentate. At 99.7 mol% ethanol in the retentate, we have only an efficiency of 10% confirming that PV is not very efficient for sharp splits. The resulting maximum of the thermodynamic efficiency is caused by the real work of the intermediate heating, which is dominant in this case, as depicted in the overview of the real work contributions in the Supplementary Information (Section A.3). With higher temperatures, the real work for intermediate heating increases, resulting in decreasing thermodynamic efficiencies. Additionally, the preheating term also rises. For a water composition in the permeate of 90 mol%, the thermodynamic efficiency drops significantly to about 21% with no distinct maximum. This is caused by the contribution of the condensation work to the real work. For a pure permeate, the condensation temperature is 32°C, while for the impure permeate, the condensation temperature is 24°C, as the more volatile component has to be condensed. This results in a positive condensation work which increases the real work of separation. The results illustrate that the membrane selectivity has a direct and potentially significant effect on the thermodynamic efficiency. Thus, the

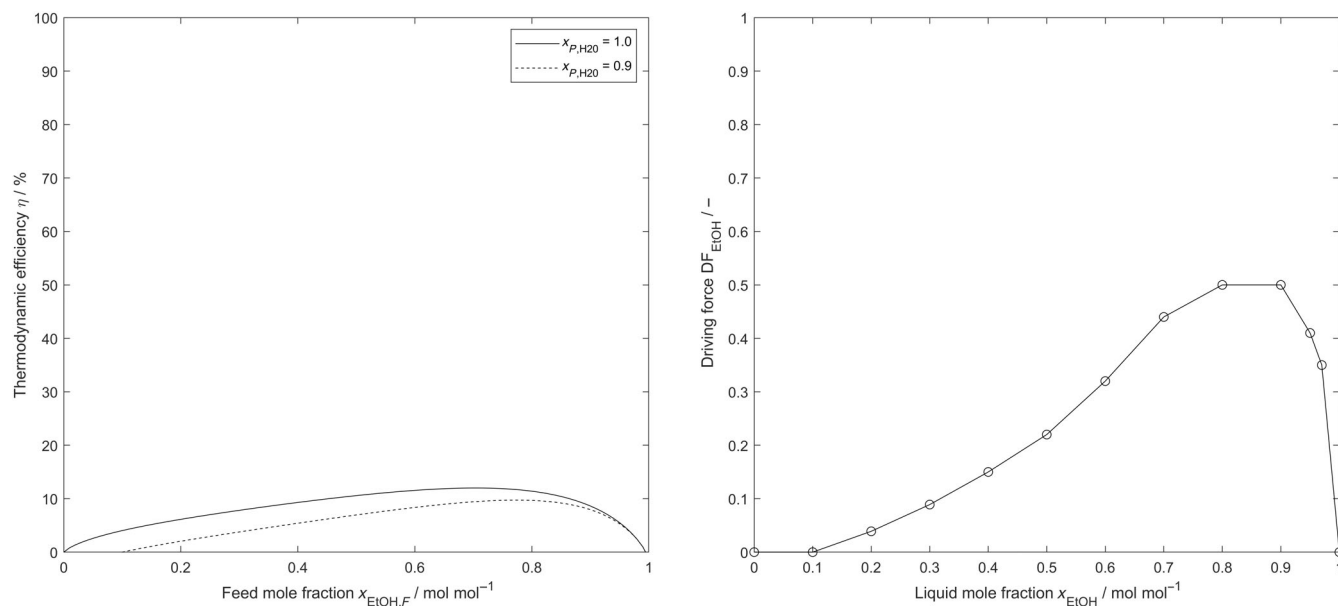


FIGURE 10 Thermodynamic efficiency (left) and driving force according to Bek-Pederson and Gani¹² (right) of a stand-alone PV of ethanol and water for different feed compositions with $x_{\text{EtOH},R} = 0.995$, $p_P = 50$ mbar $T_0 = 298.15$ K, $p_0 = 1.013$ bar, $\dot{n}_F = 100$ mol s⁻¹

increased costs of highly selective membranes, such as the frequently reported tenfold increase in costs when comparing polymeric and zeolite membranes,⁴¹ may be bearable in favor of an increased efficiency and sustainability.

The influence of the feed composition on the thermodynamic efficiency is shown in Figure 10. At higher ethanol fractions of about 70 mol%, for both permeate purities, thermodynamic efficiency drops to generally low values with a maximum of about 12% and 10%, respectively. Thus, the lower the amount of water in the feed, which has to be separated, the higher the efficiency, which also confirms the expectations that membrane separations are more favorable when extracting a smaller fraction of the feed stream. However, this requires a highly selective membrane since the driving force for mass transfer of the preferred permeating species decreases with a decrease of the species composition in the feed. The general trend for the dependency of the thermodynamic efficiency from the feed composition is however independent from the permselectivity.

Bek-Pedersen and Gani¹² also investigated the driving force for PV as illustrated in Figure 10 (right). Again, the qualitative trends are in good accordance with the highest values at higher ethanol fractions of about 80 mol% showing an influence of the feed composition. Thus, as applied in real applications, PV-assisted distillation should be configured with the distillation column in front and the PV processing the top product of the distillation column.

3.2.3 | Vapor permeation

Similar to the PV process, also for the VP processes, a hydrophilic membrane is considered, such that water is the preferred permeating component, while ethanol is enriched in the retentate. The same

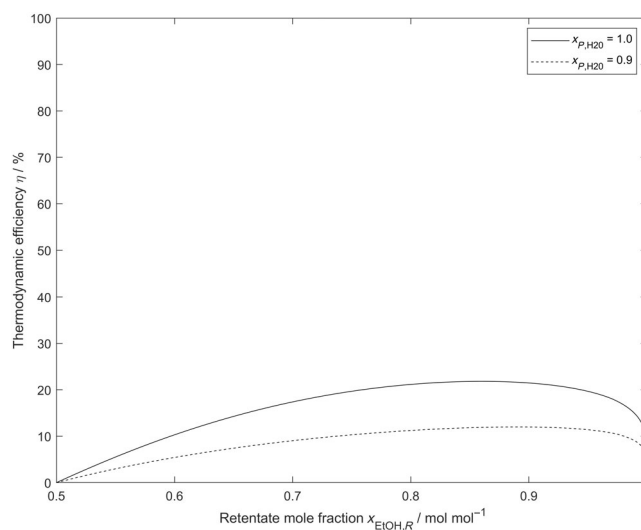


FIGURE 11 Thermodynamic efficiency of a stand-alone VP of an equimolar ethanol-water mixture for different feed compositions with a liquid feed at $T_F = 298.15$ K with $T_0 = T_F$, $p_0 = 1.013$ bar, $\dot{n}_F = 100$ mol s⁻¹

range of product compositions as shown for PV are investigated for VP.

Figure 11 illustrates the resulting thermodynamic efficiencies for which the whole feed stream first needs to be evaporated, requiring the work equivalent of the heat of evaporation as additional contribution to the real work of separation. For the high selectivity membrane with a pure permeate, a maximum of almost 22% is reached at 86 mol % ethanol in the retentate, while a maximum of only 12% is obtained for an imperfect membrane with lower purity permeate at slightly higher ethanol fractions. A pure permeate exhibits higher efficiencies

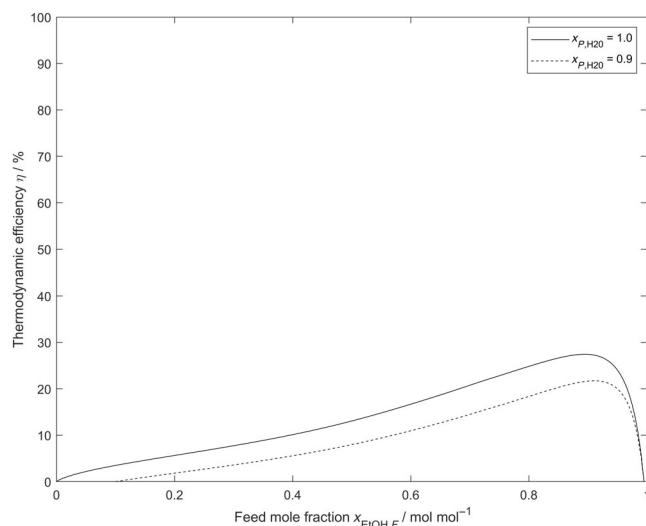


FIGURE 12 Thermodynamic efficiency of a stand-alone VP of ethanol and water for different feed compositions with $x_{\text{EtOH},R} = 0.995$, $p_P = 50$ mbar $T_0 = 298.15$ K, $p_0 = 1.013$ bar, $\dot{n}_F = 100$ mol s^{-1}

because the condensation work is lower compared to an impure permeate. For VP, the permeate purity has a great influence on efficiency and therefore the membrane selectivity should be evaluated.

In Figure 12, the influence of the feed composition on the thermodynamic efficiency is further illustrated for a fixed retentate purity of 99.5 mol% ethanol. At higher ethanol fractions of about 89 mol%, a maximum thermodynamic efficiency of 29% is reached for a high-selectivity membrane that enables a pure permeate. For an imperfect membrane with an impure permeate, a maximum of 23% is obtained, which indicates a small influence of the permeate purity on the thermodynamic efficiency.

The results show an influence of the feed composition similar to that of VP. In line with the presented conclusions, comparison of Figure 9 and Figure 13 indicates that, for the separation of a mostly aqueous up to equimolar feed, a hybrid configuration with a distillation column in front and a membrane process for ethanol purification processing the top product of the column is advantageous to operate both unit operations at high thermodynamic efficiency.

4 | INVESTIGATION OF HYBRID CONFIGURATIONS

Following the preceding analysis of the individual unit operations, the thermodynamic efficiency of different membrane-assisted hybrid processes is investigated for two representative case studies. The first case study follows the previously considered separation of a binary mixture of ethanol and water. One feed composition is considered within this manuscript and another one is given in the Supplementary Information (Section C). Second, the separation of tetrahydrofuran (THF) from a feed mixture with methanol and water is examined, representing another case study of industrial relevance.

Both case studies have already been subject to previous investigations for a techno-economical optimization for which hybrid processes were assessed with respect to MED and TAC.^{8,14,15} In these investigations, the MED was calculated as the minimum sum of the reboiler duties of the distillation columns and the energy requirement for the evaporation of the permeate for the PV unit.¹⁵ Thus, the actual temperature at which the individual heat streams had to be provided was not considered. The TAC were determined from a superstructure optimization with respect to sizing and costing models, reflecting both operating and capital cost. In the following, the results of the MED and TAC analysis are evaluated with respect to the derived thermodynamic efficiencies of the considered process variants for each case study.

To determine the thermodynamic efficiency for the hybrid configurations, the condenser and reboiler duties, which are necessary to describe the real work of the distillation column, are determined by an optimization of the overall energy demand of the hybrid process accounting for the integration of the involved unit operations, subject to the desired product specifications. Distillation columns are described analogously to Section 2.3.2 while the membrane processes are evaluated under the assumption of a (nearly) perfect membrane, according to Sections 2.3.3 and 2.3.4. The reference state is set to a temperature of 298.15 K and a pressure of 1.013 bar.

4.1 | Case study 1: Separation of ethanol and water

The first case study analyzes the dehydration of an aqueous ethanol mixture with a feed stream of 500 mol s^{-1} with 10 mol% ethanol, which is purified into 99.5 mol% ethanol and 99.9 mol% water. For this separation, three different process configurations: (1) a perfectly selective PV unit, (2) a PV-assisted distillation process with the membrane unit as polishing step for the distillate (cf. Figure 13) and (3) a heteroazeotropic distillation (HAD) with cyclohexane as entrainer (benchmark process), were investigated by Scharzec et al.¹⁵ in terms of MED. Based on this analysis, a further cost optimization was conducted for the benchmark process and the PV-assisted configuration. Thermodynamic calculations are conducted according to Section 3. Another viable benchmark process option is extractive distillation (ED), which is for certain feed compositions even superior to HAD. However, Waltermann et al.⁴² demonstrate that HAD with cyclohexane is superior to ED with ethylene glycol for a low-concentrated aqueous ethanol feed, while ED becomes favorable the higher the ethanol concentration is.

Assuming a perfectly selective membrane with only water permeating through the membrane, the permeate can directly be mixed with the bottom stream of the distillation column. For a lower permselectivity with a permeate with 10 mol% ethanol, the permeate stream is recycled to the lower part of the distillation column for further purification. The permeate pressure is assumed to 30 mbar for both scenarios.

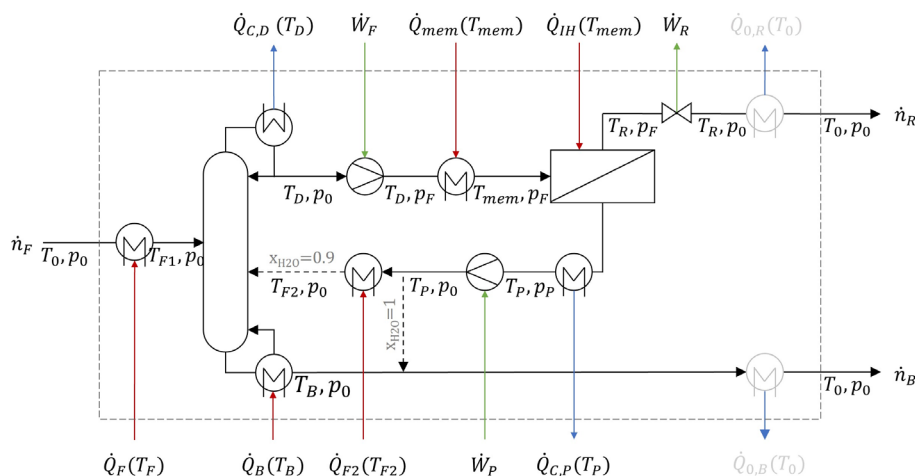


FIGURE 13 Schematic of a hybrid process (worst case) combining distillation and PV with all heat and work streams contributing to the real work related to its surroundings at reference state considering two different treatments of the permeate stream depending on the composition. Gray heat exchangers do not contribute to the real work.

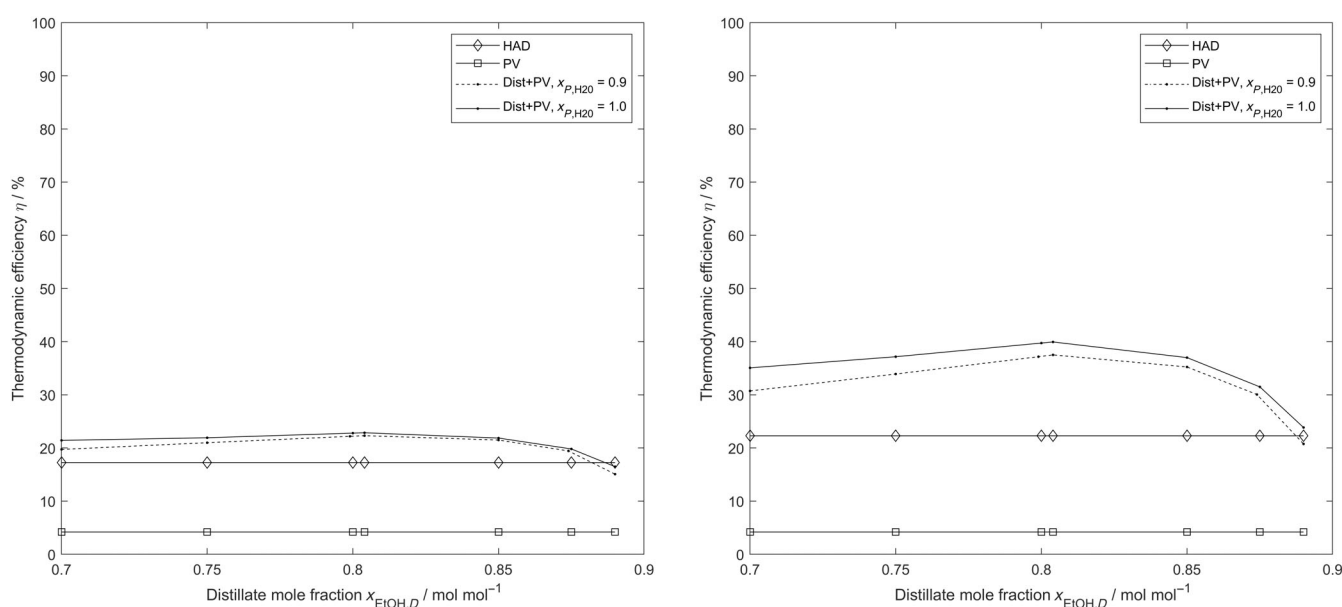


FIGURE 14 Thermodynamic efficiency for the worst-case scenario (left) and minimum energy demand¹⁵ (right) for different distillate compositions with $x_{EtOH,R} = 0.995$, $x_{H2O,B} = 0.999$, $T_0 = 298.15$ K, $p_0 = 1.013$ bar, $\dot{n}_F = 500$ mol s⁻¹

For the subsequent analysis, again a worst—no heat integration for preheating and product cooling—and a best-case—full integration—efficiency for the hybrid process are considered. The latter one is given in the Supplementary Information (Section B). To analyze the PV-assisted distillation process, the thermodynamic efficiency is evaluated for different ethanol fractions in the distillate, for which the results are shown in Figure 14 for the worst case (left) and the respective MED on the right.

It is interesting to note that unlike the stand-alone PV process, the selectivity of the membrane does barely affect the MED or thermodynamic efficiency of the hybrid process. Thus, almost the same optimum of 23% at a distillate composition of 80.4 mol % ethanol is achieved. This is because the main contributions to the real work are the column preheating and the heat duty provided in the reboiler, which are similar in both cases. The preheating of the permeate recycle stream in case of an impure permeate

has only a minor effect. The respective flowsheets and related heat input values are depicted in the Supplementary Information (Section B). With increasing ethanol content in the distillate, the thermodynamic efficiency decreases until the azeotropic point impedes the separation by distillation. The decrease in thermodynamic efficiency relates to the steep increase in MED (cf. Figure 14, right).

The thermodynamic efficiency of the PV-assisted distillation process is considerably larger compared to the HAD (17%) and the stand-alone PV process with perfectly selective membranes (4%), which highlights the benefits of the hybrid process. For HAD, the main contribution to the real work is the heat duty in the column reboilers, especially that of the first column. The ranking according to the thermodynamic efficiency is in line with the ranking according to the MED and the maximum in thermodynamic efficiency corresponds to the minimum in MED. Thus, in this case, the thermodynamically optimal

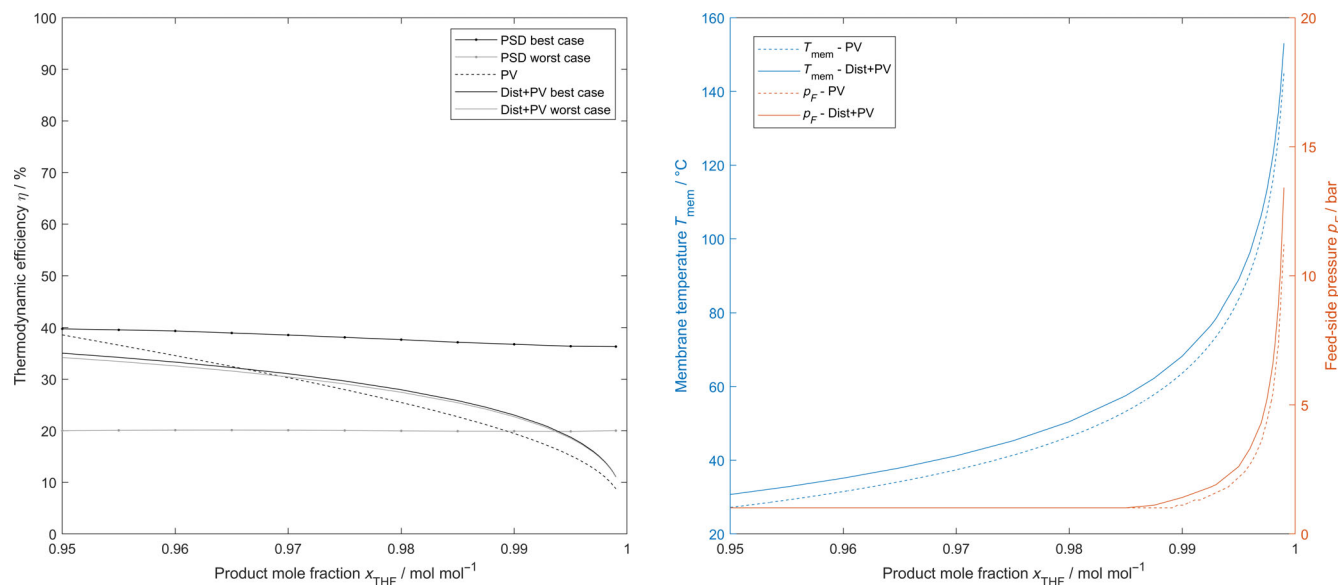


FIGURE 15 Thermodynamic efficiency (left) and resulting membrane operating conditions for the best-case scenario (right) of the considered process variants for a THF-methanol-water mixture for different product mole fractions of THF at $T_{F0} = 298.15$ K, $p_0 = 1.013$ bar, $\dot{n}_F = 10$ mol s⁻¹

distillate composition of the hybrid process can in fact be identified directly from the MED analysis.

The hybrid membrane process is the most promising variant in case of a distillate composition <88 mol%. Otherwise, the HAD process shows a comparable efficiency and MED, respectively, while the standalone PV unit cannot compete. However, the techno-economical optimization¹⁵ reveals that the TAC of the hybrid process of 3.8 mio. € a⁻¹ significantly exceed the TAC of the HAD with 2.9 mio. € a⁻¹, despite the indicated energy savings. This illustrates the importance of a combined consideration of energy efficiency and process economics. The main reason for the high cost of the membrane-assisted distillation process are in this case the need for an expensive cooling brine to operate at the low permeate pressure of 30 mbar, which accounts for one third of the TAC. The expensive utility can be avoided by operation at increased permeate pressure, which however results in a lower driving force and increased membrane area.

4.2 | Case study 2: Separation of tetrahydrofuran, methanol, and water

In the second case study, a ternary azeotropic mixture of tetrahydrofuran (THF), methanol and water is investigated, considering a feed stream of 10 mol s⁻¹ with a composition of 45 mol% THF, 40 mol% methanol and 15 mol% water, as considered by Scharzec et al.⁸ However, unlike the initial study, which assumed a liquid boiling feed, the feed stream is considered at ambient temperature and pressure. The separation is supposed to obtain THF with a purity of 99.9 mol% and a recovery of 99.9%. As the focus of the separation is on THF purification, water and methanol are not separated further, and thus only two product streams are considered.

Thermodynamic calculation are conducted according to Scharzec et al.,⁸ which the Gibbs triangle is provided in the Supplementary Information in Section D.

For this case study, a PV unit (cf. Figure 4) and a PV-assisted processes (cf. Figure 13) are evaluated in comparison to a PSD process as a benchmark process. The results of the previous MED and techno-economic optimization⁸ serve as the basis of the thermodynamic efficiency analysis in the current study, which furthermore considers the necessary preheating and evaluates different product purities. The MED of the standalone PV process is approximated with a perfectly selective membrane, which operates at a permeate pressure of 30 mbar. While this provides an interesting best-case approximation for a standalone PV process, which basically requires an almost perfectly selective membrane to enable such high purities and recoveries, no such membranes is currently available. Therefore, for the MED evaluation of the PV-assisted hybrid process, an imperfect membrane that retains 95% THF is considered. The first distillation column is operated at 0.4 bar vacuum, and thus a pressure reduction has to be considered for the calculation of the real work.

Under these considerations, the PV-assisted process shows a slightly lower MED (520 kW) than the heat-integrated PSD (569 kW). However, the PV-assisted process results in significantly higher TAC (793 vs. 223 k€ a⁻¹).⁸ The techno-economic optimization revealed that the limited performance of the hybrid process is mainly caused by the high purity and recovery requirements for THF. For this reason, we investigate the thermodynamic efficiency of the mentioned processes on the basis of re-optimized processes for MED for different product purities in the range of 95–99.9 mol% THF. The resulting thermodynamic efficiencies are illustrated in Figure 15 (left) in line with the determined temperatures and pressures for the membrane separation according to Section 2.3.3, cf. Figure 15 (right).

Considering the PSD process without explicit modeling of the heat integration, a thermodynamic efficiency of around 20% for the worst case, and 38% for the best-case approximation (ideal heat integration between product/recycle streams and feed heating, as well as beneficial use of condenser heats), is calculated. These values are almost independent of the THF purity. While an ideal PV-based separation would enable a thermodynamic efficiency of about 38.5% for 95% THF purity, the thermodynamic efficiency of the PV as well as the PV-assisted process drop to 9% and 11% for a THF purity of 99.5%, respectively. Even if a perfectly selective membrane would be available, the purity specifications would mandate a feed temperature of 145°C at 11 bar feed-side pressure for the stand-alone PV separation in order to maintain a positive driving force, which is significant beyond the range of 100°C and 4 bar for polymeric membranes,⁴³ and even at the limit of 150°C and 10 bar for inorganic membranes, for example, hybrid silica membrane.⁴⁴ No such membrane with a sufficient performance is currently available.⁸

Overall, the membrane-assisted processes are less efficient compared to the best-case PSD process highlighting the importance of heat integration. The better performance of the PSD process is also confirmed by the results of the techno-economic optimization of Scharzec et al.,⁸ which explicitly considers the heat integration of the PSD process.

5 | CONCLUSION

Although frequently recited, membrane separations are not generally more energy efficient compared to distillation and potential savings of up to 90%⁴⁵ are rarely reached. This was recently illustrated by Chavez Velasco et al.³³ for p-xylene/o-xylene and propylene/propane separations and is further confirmed in the current study by investigation of the thermodynamic efficiency of pervaporation and vapor permeation processes in comparison to distillation as well as membrane-assisted distillation processes for the important case of alcohol dehydration.

The analysis of the thermodynamic efficiency of the standalone processes confirms the previously reported results for distillation processes,^{21,22,26} highlighting the possibly high internal efficiencies for distillation-based separation, if heat integration between feed and product/recycle streams is pursued and the heat of condensation is utilized beneficially. Especially for feed streams with a lower fraction of low-boiling components high efficiencies are feasible. For pervaporation and vapor permeation, especially the feed and product purities as well as the membrane selectivity are important factors affecting the thermodynamic efficiency. Under the assumption of an optimal heat integration, distillation potentially outperform pervaporation or vapor permeation in terms of the thermodynamic efficiency for a range of feed and product specifications. Unlike the distillation-based separations, the thermodynamic efficiency of the membrane separations drops significantly with increasing product recovery and purity. As illustrated in the current study, hybrid combinations of membrane-assisted distillation processes bear the potential to further improve the energy efficiency, while reducing the need for heat integration.

While the conducted study allows for an effective analysis of the different process concepts with respect to the thermodynamic efficiency, it has to be pointed out that the reported efficiencies are reflecting internal efficiencies under ideal assumptions, which especially include the beneficial use of dissipated heat, as well as the negligence of losses in the heat exchangers and heat losses in the unit operations. These additional losses can lead to a significant reduction of the thermodynamic efficiency, which is however not caused by the separation process, but the overall energy integration, insulation, and design of heat exchangers.

Comparing the results of the current exergy-based evaluation of the different process concepts, with previously conducted techno-economic process optimization studies, it becomes apparent that the latter is especially important for material-intensive processes, such as the considered membrane separations, but also processes such as adsorption. Although the results of the energy-based and efficiency-based evaluation are quite similar for the current investigations, this similarity results from the majority of the real work being grounded in thermal contributions. These results may be considerably different if mechanical work, for example, for vapor recompression, or pressure-driven membrane processes are considered. These considerations are therefore to be evaluated in future work, which also should consider a multi-criteria optimization with respect to energy, efficiency, and costs.

AUTHOR CONTRIBUTIONS

Bettina Kruber: Conceptualization (equal); investigation (lead); methodology (equal); software (lead); writing – original draft (lead); writing – review and editing (equal). **Karen Droste:** Investigation (supporting); methodology (supporting); software (supporting). **Mirko Skiborowski:** Conceptualization (equal); investigation (supporting); methodology (equal); supervision (lead); writing – review and editing (equal).

ACKNOWLEDGMENT

Open Access funding enabled and organized by Projekt DEAL.

DATA AVAILABILITY STATEMENT

The data that support the findings of this study are available from the corresponding author upon reasonable request.

ORCID

Bettina Kruber  <https://orcid.org/0000-0003-2638-9803>

REFERENCES

1. Franke M, Górak A, Strube J. Auslegung und Optimierung von hybriden Trennverfahren. *Chem Ing Tech*. 2004;76(3):199-210.
2. Lipnizki F, Field RW, Ten P-K. Pervaporation-based hybrid process: a review of process design, applications and economics. *J Membr Sci*. 1999;153(2):183-210.
3. Kreis P, Górak A. Process analysis of hybrid separation processes: combination of distillation and pervaporation. *Chem Eng Res Des*. 2006;84(7):595-600.
4. Skiborowski M, Harwardt A, Marquardt W. Conceptual design of distillation-based hybrid separation processes. *Annu Rev Chem Biomol Eng*. 2013;4:45-68.

5. Drioli E, Stankiewicz AI, Macedonio F. Membrane engineering in process intensification—an overview. *J Membr Sci*. 2011;380(1–2):1–8.
6. Suk DE, Matsuura T. Membrane-based hybrid processes: a review. *Sep Sci Technol*. 2006;41(4):595–626.
7. Fontalvo J, Cuellar P, Timmer JMK, Vorstman MAG, Wijers JG, Keurentjes JTF. Comparing pervaporation and vapor permeation hybrid distillation processes. *Ind Eng Chem Res*. 2005;44(14):5259–5266.
8. Scharzec B, Merschhoff D, Henrichs J, Kappert EJ, Skiborowski M. Evaluation of membrane-assisted hybrid processes for the separation of a tetrahydrofuran-methanol–water mixture. *Chem Eng Process Process Intensif*. 2021;167:108545.
9. Vane LM. Review of pervaporation and vapor permeation process factors affecting the removal of water from industrial solvents. *J Chem Technol Biotechnol*. 2020;95(3):495–512.
10. Liu S, Li H, Kruber B, Skiborowski M, Gao X. Process intensification by integration of distillation and vapor permeation or pervaporation—an academic and industrial perspective. *Results Eng*. 2022;15:100527.
11. Bek-Pedersen E, Gani R, Levaux O. Determination of optimal energy efficient separation schemes based on driving forces. *Comput Chem Eng*. 2000;24(2–7):253–259.
12. Bek-Pedersen E, Gani R. Design and synthesis of distillation systems using a driving-force-based approach. *Chem Eng Process Process Intensif*. 2004;43(3):251–262.
13. Bausa J, Marquardt W. Shortcut design methods for hybrid membrane/distillation processes for the separation of nonideal multicomponent mixtures. *Ind Eng Chem Res*. 2000;39(6):1658–1672.
14. Skiborowski M, Wessel J, Marquardt W. Efficient optimization-based design of membrane-assisted distillation processes. *Ind Eng Chem Res*. 2014;53(40):15698–15717.
15. Scharzec B, Waltermann T, Skiborowski M. A systematic approach towards synthesis and design of pervaporation-assisted separation processes. *Chem Ing Tech*. 2017;89(11):1534–1549.
16. Bausa J, Watzdorf R, Marquardt W. Minimum energy demand for nonideal multicomponent distillations in complex columns. *Comput Chem Eng*. 1996;20:55–60.
17. Seider WD, Lewin DR, Seader JD, Widagdo S, Gani R, Ng KM. *Product and Process Design Principles: Synthesis, Analysis and Evaluation*. 4th ed; 2016, Wiley.
18. Rant Z. Ein neues Wort für technische Arbeitsfähigkeit. *Forschung Auf Dem Gebiet Des Ingenieurwesens*. 1956;22:36–37.
19. Demirel Y. Thermodynamic analysis of separation systems. *Sep Sci Technol*. 2004;39(16):3897–3942.
20. Agrawal R, Woodward DW. Efficient cryogenic nitrogen generators: an exergy analysis. *Gas Sep Purif*. 1991;5(3):139–150.
21. Agrawal R, Herron DM. Optimal thermodynamic feed conditions for distillation of ideal binary mixtures. *AIChE J*. 1997;43(11):2984–2996.
22. Bandyopadhyay S. Effect of feed on optimal thermodynamic performance of a distillation column. *Chem Eng J*. 2002;88(1–3):175–186.
23. Agrawal R, Fidkowski ZT. Are thermally coupled distillation columns always thermodynamically more efficient for ternary distillations? *Ind Eng Chem Res*. 1998;37(8):3444–3454.
24. Kencse H, Mizsey P. Methodology for the design and evaluation of distillation systems: exergy analysis, economic features and GHG emissions. *AIChE J*. 2010;56(7):1776–1786.
25. Kiss AA, Olujić Ž. A review on process intensification in internally heat-integrated distillation columns. *Chem Eng Process Process Intensif*. 2014;86:125–144.
26. Tumbalam Gooty R, Chavez Velasco JA, Agrawal R. Methods to assess numerous distillation schemes for binary mixtures. *Chem Eng Res Des*. 2021;172:1–20.
27. Blahušiak M, Kiss AA, Kersten S, Schuur B. Quick assessment of binary distillation efficiency using a heat engine perspective. *Energy*. 2016;116:20–31.
28. Brogioli D, La Mantia F, Yip NY. Thermodynamic analysis and energy efficiency of thermal desalination processes. *Desalination*. 2018;428:29–39.
29. Xu J, Agrawal R. Membrane separation process analysis and design strategies based on thermodynamic efficiency of permeation. *Chem Eng Sci*. 1996;51(3):365–385.
30. Cussler EL, Dutta BK. On separation efficiency. *AIChE J*. 2012;58(12):3825–3831.
31. Castel C, Favre E. Membrane separations and energy efficiency. *J Membr Sci*. 2018;548:345–357.
32. Agrawal R, Tumbalam GR. Misconceptions about efficiency and maturity of distillation. *AIChE J*. 2020;66(8):195.
33. Chavez Velasco JA, Tawarmalani M, Agrawal R. Systematic analysis reveals thermal separations are not necessarily most energy intensive. *Joule*. 2021;5(2):330–343.
34. Ishida M, Nakagawa N. Exergy analysis of a pervaporation system and its combination with a distillation column based on an energy utilization diagram. *J Membr Sci*. 1985;24(3):271–283.
35. King CJ. *Separation Processes*. McGraw-Hill Chemical Engineering Series. 2nd ed. McGraw-Hill; 1980.
36. Melin T, Rautenbach R. *Membranverfahren: Grundlagen der Modul- und Anlagenauslegung*. 3rd ed. Springer; 2007.
37. Wynn N. Pervaporation comes of age. *Chem Eng Process*. 2001;97:66–72.
38. Posada JA, Patel AD, Roes A, Blok K, Faaij APC, Patel MK. Potential of bioethanol as a chemical building block for biorefineries: preliminary sustainability assessment of 12 bioethanol-based products. *Bioresour Technol*. 2013;135:490–499.
39. Lai H-S, Lin Y-F, Tu C-H. Isobaric (vapor + liquid) equilibria for the ternary system of (ethanol + water + 1,3-propanediol) and three constituent binary systems at $P = 101.3$ kPa. *J Chem Thermodyn*. 2014;68:13–19.
40. Skiborowski M, Harwardt A, Marquardt W. Efficient optimization-based design for the separation of heterogeneous azeotropic mixtures. *Comput Chem Eng*. 2015;72:34–51.
41. Vane LM. Review: membrane materials for the removal of water from industrial solvents by pervaporation and vapor permeation. *J Chem Technol Biotechnol*. 2019;94(2):343–365.
42. Waltermann T, Grueters T, Muenchrath D, Skiborowski M. Efficient optimization-based design of energy-integrated azeotropic distillation processes. *Comput Chem Eng*. 2020;133:106676.
43. DeltaMem AG. *Membrane Data Sheet: PERVAP Polymeric Membranes*. DeltaMem AG; 2016.
44. PERVATECH. *Datasheet: Hybrid Silica HybSi(R) AR Membranes*. Pervatech BV; 2018.
45. Sholl DS, Lively RP. Seven chemical separations to change the world. *Nature*. 2016;532(7600):435–437.

SUPPORTING INFORMATION

Additional supporting information can be found online in the Supporting Information section at the end of this article.

How to cite this article: Kruber B, Droste K, Skiborowski M. Thermodynamic efficiency of membrane-assisted distillation processes. *AIChE J*. 2023;e18015. doi:10.1002/aic.18015